Brief Communication

Experimental Observation of Pulsating Instability under Acoustic Field in Downward-Propagating Flames at Large Lewis Number

Sung Hwan YOON[1, 3], Longhua HU[2], Osamu FUJITA[1*]

[1] Division of Mechanical and Space Engineering,
Hokkaido University
Kita13 Nishi 8, Kita-ku, Sapporo 060-8628, Hokkaido, Japan

[2] State Key Laboratory of Fire Science,
University of Science and Technology of China,
Hefei, Anhui 230026, China

[3] Current address: Clean Combustion Research Center
King Abdullah University of Science and Technology
Thuwal 23955-6900, Saudi Arabia

*Corresponding author: Tel: (+81) 11 7066385; Fax: (+81) 11 7067841;
Email address: ofujita@eng.hokudai.ac.jp;
Postal address: Hokkaido University, Kita13 Nishi 8, Kita-ku, Sapporo 060-8628, Hokkaido, Japan

Abstract

According to previous theory, pulsating propagation in a premixed flame only appears when the reduced Lewis number, $\beta(Le-1)$, is larger than a critical value (Sivashinsky criterion: $4(1+\sqrt{3}) \approx 11$), where β represents the Zel'dovich number (for general premixed flames, $\beta \approx 10$), which requires Lewis number $Le > 2.1$. However, few experimental observation have been reported because the critical reduced Lewis number for the onset of pulsating instability is beyond what can be reached in experiments. Furthermore, the coupling with the unavoidable hydrodynamic instability limits the observation of pure pulsating instabilities in flames. Here, we describe a novel method to observe the pulsating instability. We utilize a thermoacoustic field caused by interaction between heat release and acoustic pressure fluctuations of the downward-propagating premixed flames in a tube to enhance conductive heat loss at the tube wall and radiative heat loss at the open end of the tube due to extended flame residence time by diminished flame surface area, i.e. flat flame. The thermoacoustic field allowed pure observation of the pulsating motion since the primary acoustic force suppressed the intrinsic hydrodynamic instability resulting from thermal expansion. By employing this method, we have provided new experimental observations of the pulsating instability for premixed flames. The Lewis number (i.e., $Le \approx 1.86$) was less than the critical value suggested previously.

Keywords

Acoustic instability; Combustion instability; Diffusive-thermal instability; Lewis number; Pulsating instability.

1. Introduction

Premixed gas combustion is intrinsically unstable due to (1) the hydrodynamic instability [1] caused by the density difference between unburned and burned mixtures and (2) the diffusive-thermal instability [2] caused by the imbalance between the mass and thermal diffusivities of the unburned mixture. In particular, the diffusive-thermal instability can result in different types of instability phenomena which are cellular and pulsating instabilities depending on Lewis number (*Le*). According to the dispersion relation for the adiabatic flame obtained from a linear stability analysis [2], the cellular instability, which is caused by focusing and diverging mass diffusion at the wrinkled flame, takes place when *Le* is smaller than a critical value, $Le_c = 1\text{-}2/\beta$. For a general premixed flame, $\beta \approx 10$, thus $Le_c = 0.8$. The pulsating instability appears when the reduced Lewis number, $\beta(Le\text{-}1)$, is larger than the Sivashinsky criterion ($4(1+\sqrt{3}) \approx 11$) [2], or $Le > 2.1$. Joulin and Clavin [3] later showed that excessive heat loss can significantly reduce the critical value of the reduced Lewis number to 6 ($Le > 1.6$) for the onset of pulsating instability in non-adiabatic flames along with constant density to eliminate hydrodynamic instability.

Concerning the experimental studies, the cellular instability can be easily observed based on Markstein's work [4]. For the pulsating instability, however, the thermo-diffusive analyses based on a one-step model [2, 3] cannot be applied directly to real flames since (1) the threshold values of β and *Le* are beyond the range that can be attained in premixed combustion experiments and (2) the hydrodynamic instabilities dominate the thermo-diffusive effects at long wavelength perturbations [5]. Although traveling wave instabilities with similar pulsating motions, such as spiral wave and target patterns, were observed in a few studies [6, 7], the dynamic mechanisms were not clear because the pulsating behaviors were combined in these experiments with hydrodynamic instabilities. A clear observation of a pure pulsating instability was difficult to accomplish experimentally.

To solve this problem, we utilized the sustained thermoacoustic field, as a state of nature for a premixed flame propagating in an open-ended tube [8-12]. Since the acoustic field formed by the interaction between heat released by the flame and acoustic fluctuations suppresses the hydrodynamic instability, it enables observation of the pure pulsating instability. Furthermore, the vibrating flat flame created by the primary acoustic instability strengthens heat losses for several reasons. First, the longer

residence time for flame propagation due to the diminished displacement velocity caused by relatively smaller flame surface area of the flat flame than curved shape, enhances the conductive heat loss at the tube wall; meanwhile the radiative heat loss at the open end of the tube is also increased. Second, the dynamic contact of the flame edge with the tube wall increases the conductive heat loss through the back-and-forth motion of combustion gas.

This article reports a clearer observation of the pulsating instability than previous studies [6, 7] in the absence of the hydrodynamic instability by applying the primary acoustic field accomplished by the above experimental method at $Le \approx 1.86$.

2. Experiments

The propagation tube (50 mm inner diameter, 711 mm length) was fixed vertically and charged with a premixed gas at atmospheric pressure. The tested premix gases were propane, oxygen and nitrogen at two fixed equivalence ratios of 0.8 and 1.2 but various laminar burning velocities, to produce reduced Le, $\beta(Le\text{-}1)$, as summarized in Table 1. When the spark igniter was activated near the upper end of the tube, the top lid was simultaneously opened automatically. The time-dependent downward-propagating flame was recorded by two high-speed cameras. The high-speed cameras captured the side view and the inclined bottom view of the propagating flame. The temporal pressure variation was measured with a dynamic pressure sensor located at the bottom end of the tube. The detailed experimental procedure and mixture properties can be found in Supplementary Material.

3. Results and Discussion

Figure 1 shows typical flame transition behaviors in a spontaneously generated acoustic field. The numerical values at the left hand side of the picture indicate the distance from the upper end of the tube. Six distinct types of flame transitions were identified with variation of S_L or reduced Le, $\beta(Le\text{-}1)$:

I: Non-vibrating curved flame

II: Curved → Vibrating curved flame

III-1: Curved → Vibrating flat flame

III-2: Curved → Flat → Pulsating instability with acoustic vibration

IV: Curved → Flat → Corrugated → Turbulent

V: Curved → Corrugated → Turbulent

The flame behavior of Regime III-2 corresponding to the pulsating instability is not included in Fig. 1. The detail will be shown later in Fig. 2. When S_L was low in lean flames, a regime of non-vibrating flame (Regime I) in which the curved flame propagated without velocity fluctuation was identified. However, this regime was only observed in lean flames, because rich flames have relatively low *Le* (Φ = 0.8; *Le* ≈ 1.86 and Φ = 1.2; *Le* ≈ 1.04) and these are very sensitive to acoustic fluctuations even with very small S_L [12]. When S_L was low in rich flames, a regime of acoustic instability (Regime II) was identified in which the flame fronts were still curved, however, non-constant acoustic vibration showed up with small acoustic sound. It was noted that the amplitude of the acoustic pressure fluctuation was not saturated during flame travel to the bottom of the tube according to the pressure measurement. When S_L was increased, vibrating flat flames appeared with relatively amplified acoustic sound (Regime III). This was a representative process of primary acoustic instability and the acoustic pressure could be saturated [8, 11]. Also, the primary acoustic field suppressed the initial hydrodynamic instability as observed in Fig. 1. When S_L was further increased, the vibrating flames finally resulted in turbulent motions via corrugated structures with violent acoustic sound (Regime IV). This was a typical process of secondary acoustic instability [13]. When S_L was very large, explosive turbulent motion resulted without the process of flat flames (Regime V). These transition behaviors were in accordance with previous observations [8, 11].

It was found that the mean displacement velocity of flat flame before transition to the corrugated structure in Mix. 5 (S_d = 23.4 cm/s; acoustic) was lower than in Mix. 3 (S_d = 27.7 cm/s; non-acoustic) although S_L in Mix. 5 (S_L = 27.5 cm/s) was higher than in Mix. 3 (S_L = 22.5 cm/s). This is due to the relatively small flame surface area (i.e. flat flame) caused by the primary acoustic field. According to previous study [5], the rate of heat released per unit cross-sectional area of the tube by the curved flame is proportional to the flame surface area. Therefore, the conductive and radiative heat losses in the acoustic field should be higher than in the non-acoustic field because of extended flame residence time in the tube.

Regime III-2 (pulsating instability with acoustic vibration) could be identified for lean propane mixture with $9.8 < \beta(Le\text{-}1) < 10$. Figure 2a shows sequential images of pulsating instability in Mix. 9 from the side view camera. The numerical values at the bottom of the picture indicate the elapsed time

(unit: *s*) after ignition. The initial stage of Regime III-2 after ignition was almost identical with Regime IV. However, it was not developed from the vibrating flat flame to corrugated structure as observed in Regime IV. Instead, periodic pulsation together with acoustic vibration was observed after the vibrating flat flame. This pulsation began from convex structure (i.e. pacemaker point, see Fig. 2b) located at the center of the flame surface and the pacemaker point periodically moved up and down keeping the convex shape at a frequency of the order of 1 Hz. The pacemaker point did not disappear during pulsation, in other words, it is an indicator of pulsating instability. At t = 0.6085 *s* in Fig. 2a, the pacemaker point is embedded in the flame base as an M shape and its width keeps decreasing along with the sinking motion into a trough to t = 0.645 *s*. After t = 0.645 *s*, the pacemaker point starts to escape out of the trough located nearby itself. At t = 0.719 *s*, the pacemaker point is slightly projected from the flame base, after then, it restarts to sink. This periodic flame motion repeated twice during flame propagation to the bottom of the tube. Such motion was never found for lean and rich methane flames (Le = 0.96 and 1.1, respectively) according to our additional experiments.

Figure 3 shows sequential images taken from below of the flames in Regime III-1 (upper) and in Regime III-2 (lower). These correspond to Mix. 15 and Mix. 9, respectively. The numerical values at the bottom of each picture show the elapsed time (unit: *s*) after ignition. It can be clearly seen from the comparison that there is a distinct difference between the saturated primary acoustic instability (Mix. 15; Regime III-1) and the pulsating instability along with the primary acoustic vibration (Mix. 9). In Regime III-2, the repeated shrinking and enlargement motion of the pacemaker point is observed. Furthermore, the vibration frequency of Regime III-1 (Mix. 15) was 145.47 Hz based on flame movement caused by primary acoustic vibration (which is confirmed by the measured acoustic pressure fluctuation: 145.85 Hz). On the other hand, for Regime III-2, two characteristic vibration frequencies based on flame movement were observed at 4.67 Hz and 177.9 Hz. The high frequency motion is caused by primary acoustic vibration [8, 11]. The low frequency motion is dominated by the pulsating instability since this instability could be only observed at Le > 1. However, in the acoustic pressure measurement, only the single characteristic frequency was found at 173.4 Hz in Regime III-2, whose value is similar to that of the high frequency motion (177.9 Hz) caused by primary acoustic vibration.

Also, it is important to note that Regime III-2 (with nonoccurrence of the secondary acoustic

instability) could be observed after Regime IV (with secondary acoustic instability) as S_L is further increased for lean propane flames (see Table 1). In other words, the amplitude of the generated acoustic pressure suddenly declined as S_L was increased since the secondary acoustic instability generated much higher acoustic sound than that of the primary acoustic instability. This may occur because the pulsating instability suppresses the transition to the secondary acoustic instability driven by longitudinal acoustics. This finding is different from previous studies [13], which showed that acoustic vibration developed a primary instability, a secondary instability and turbulent as S_L was increased at a constant wave number. This difference may be caused by which the Markstein number of adiabatic flames was obtained with the one-step Arrhenius model in the limit of a large activation energy in their study. More recent studies [5, 14] suggest that the old-fashioned analyses [13], have been carried out within the framework of the simplest flame model, may be extended by multiple-step models. Therefore, our experimental observations provides important information that the pulsating instability generated on the flame surface does not affect acoustic pressure fluctuation in the primary acoustic instability but could prevent transition to the turbulent motion.

4. Concluding remarks

It was found that the combustion tube experiments with spontaneous acoustic instability was effective to observe the pulsating instability because of suppressed hydrodynamic instability as well as increased heat loss from the flame to the tube wall. With the method, the pulsating instability behavior was clearly captured although the Lewis number (i.e., $Le \approx 1.86$) was approximately 10 % less than the critical value suggested by the theoretical research [2]. It was found that the pulsating instability could suppress the transition to the secondary acoustic instability.

Acknowledgments

This study was supported by a Grant-in-Aid for Scientific Research (KIBAN (B) #26289042) from MEXT Japan. The authors thank Dr. M. S. Cha for his valuable assistance.

Reference

[1] L. Landau, On the theory of slow combustion, Acta Physicochim. 19 (1944) 77-85.

[2] G. I. Sivashinsky, Diffusional-thermal theory of cellular flames, Combust. Sci. and Tech. 15 (1977) 137-145.

[3] G. Joulin, P. Clavin, Linear stability analysis of nonadiabatic flames: diffusional-thermal model, Combust. Flame 35 (1979) 139-153.

[4] G. H. Markstein, Nonsteady Flame Propagation, Pergamon (1964).

[5] P. Clavin, G. Searby, Combustion Waves and Fronts in Flows: Flames, Shocks, Detonations, Ablation Fronts and Explosion of Stars, Cambridge University Press, Cambridge, U.K. (2016).

[6] H. G. Pearlman, P. D. Ronney, Near-limit behavior of high Lewis-number premixed flames in tubes at normal and low gravity, Phys. Fluids 6 (1994) 4009-4018.

[7] H. G. Pearlman, Excitability in high-Lewis number premixed gas combustion, Combust. Flame 109 (1997) 382-398.

[8] G. Searby, Acoustic instability in premixed flames, Combust. Sci. and Tech. 81 (1992) 221-231.

[9] J. S. Park, O. Fujita, Y. Nakamura, H. Ito, Transition of flat flames to turbulent motion induced by external laser irradiation, Proc. Combust. Inst. 33, (2011) 1105-1112.

[10] Y. Taniyama, O. Fujita, Initiation and formation of the corrugated structure leading to the self-turbulization of downward propagating flames in a combustion tube with external laser absorption, Combust. Flame 161 (2014) 1558-1565.

[11] S. H. Yoon, T. J. Noh, O. Fujita, Onset mechanism of primary acoustic instability in downward-propagating flames, Combust. Flame 170 (2016) 1-11.

[12] S. H. Yoon, T. J. Noh, O. Fujita, Effects of Lewis number on generation of primary acoustic instability in downward-propagating flames, Proc. Combust. Inst. 36 (2017) 1603-1611.

[13] G. Searby, D. Rochwerger, A parametric acoustic instability in premixed flames, J. Fluid Mech. 231 (1991) 529-543.

[14] P. Clavin, J. C. Graña-Otero, Curved and stretched flames: the two Markstein numbers, J. Fluid Mech. 686 (2011), pp. 187-217.

Table 1 Summary of the properties of premixed gases and corresponding flame instability regimes.

Mix.	C_3H_8	O_2	N_2	Φ	S_L (cm/s)	$\beta(Le\text{-}1)$	Regime
1	0.027	0.169	0.804	0.8	17.5	9.82	I
2	0.028	0.175	0.797		20.0	9.72	I
3	0.029	0.182	0.789		22.5	9.76	I
4	0.030	0.188	0.782		25.0	9.84	II
5	0.031	0.194	0.775		27.5	9.85	IV
6	0.032	0.200	0.768		30.0	9.78	IV
7	0.033	0.206	0.762		32.5	9.84	IV
8	0.034	0.211	0.755		35.0	9.89	III-2
9	0.035	0.217	0.749		37.5	9.92	III-2
10	0.035	0.222	0.743		40.0	10.03	V
11	0.036	0.227	0.737		42.5	10.17	V
12	0.033	0.135	0.832	1.2	7.5	0.73	II
13	0.034	0.142	0.823		10.0	0.63	II
14	0.036	0.149	0.816		12.5	0.56	III-1
15	0.037	0.155	0.808		15.0	0.52	III-1
16	0.039	0.161	0.801		17.5	0.48	IV
17	0.040	0.166	0.794		20.0	0.45	IV
18	0.041	0.172	0.787		22.5	0.41	IV
19	0.042	0.177	0.781		25.0	0.40	V
20	0.046	0.192	0.761		32.5	0.36	V
21	0.051	0.212	0.737		42.5	0.32	V

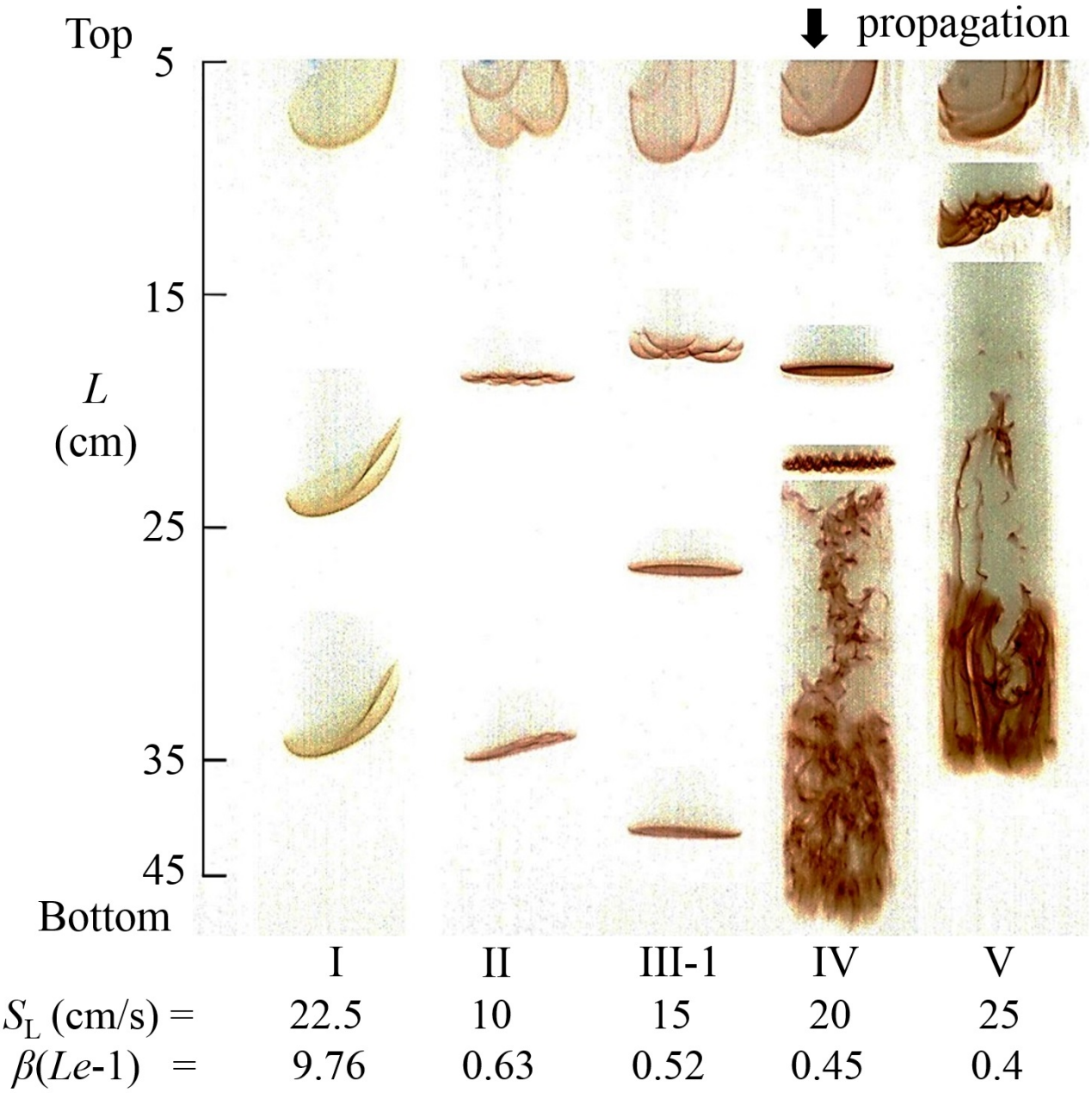

Fig. 1. The features of flame transitions in acoustic field: (I) Mix. 3, (II) Mix. 13, (III-1) M ix. 15, (IV) Mix. 17 and (V) Mix. 19.

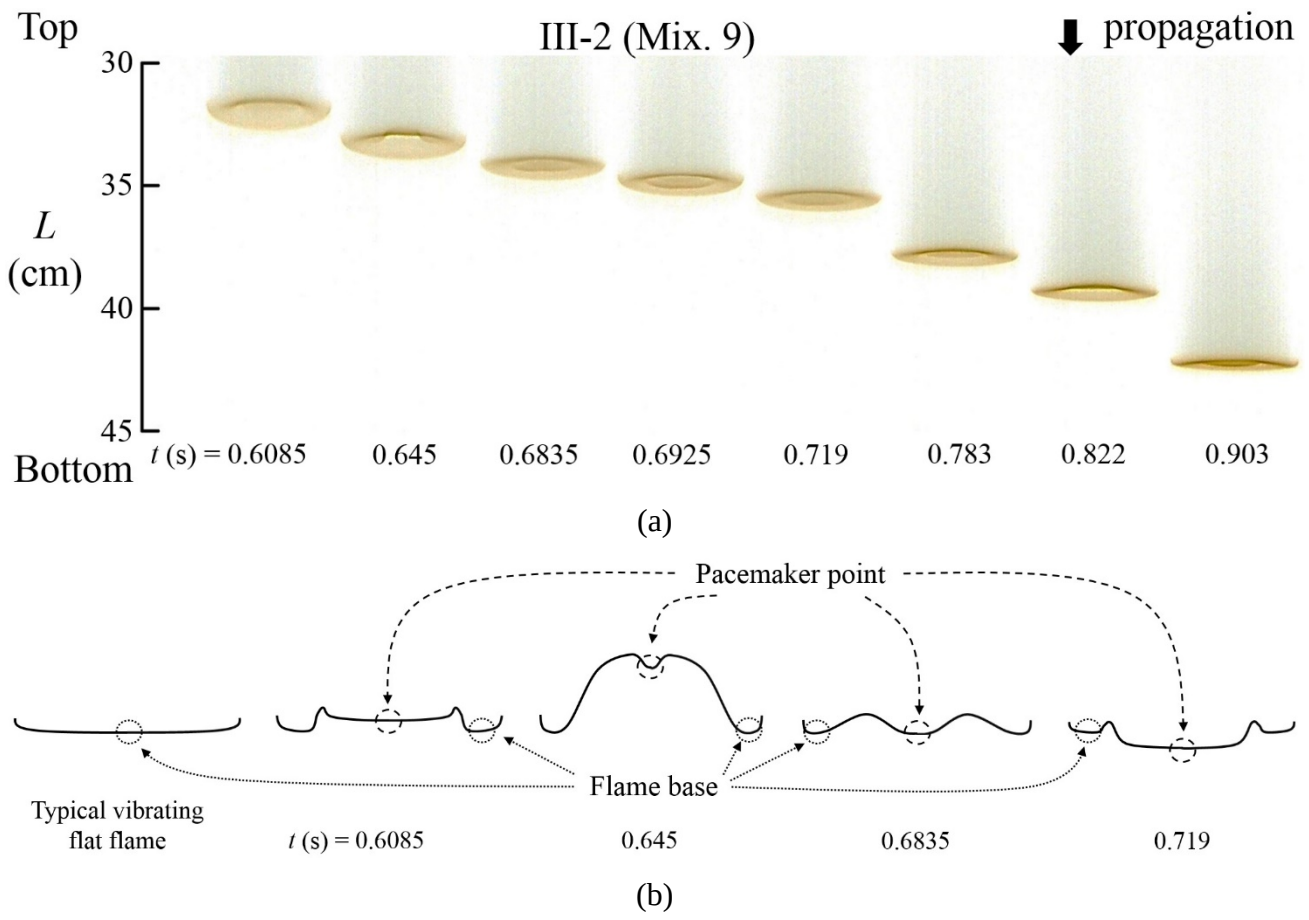

Fig. 2. (a) Sequential images (side view) for a pulsating flame in Mix. 9 (S_L = 37.5 m/s; β (*Le*-1) = 9.92) (b) Explanatory diagram of pulsating instability connected with Fig. 2a.

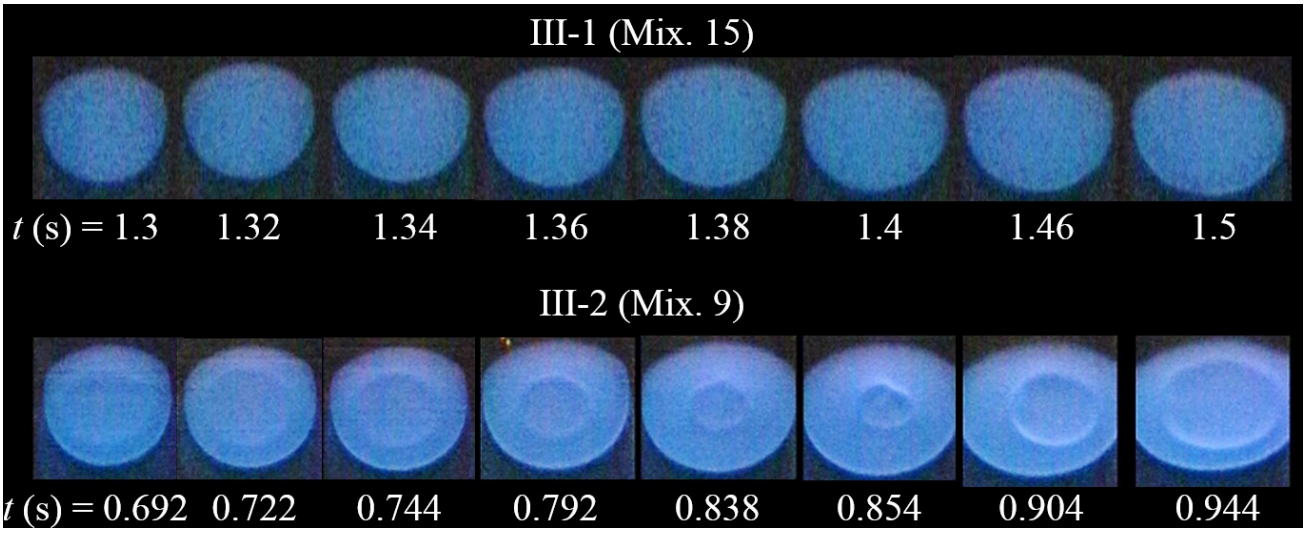

Fig. 3. Sequential images (inclined view) of the flame front in Mix. 15 (upper: S_L = 15 cm/s; $\beta(Le\text{-}1)$ = 0.52) and Mix. 9 (bottom: S_L = 37.5 cm/s; $\beta(Le\text{-}1)$ = 9.92).